Quantitative Interpretation of Petrophysical Parameters for Reservoir Characterization in an Onshore Field of Niger Delta Basin

Original Research Article

ABSTRACT

Reservoir characterization of a field was performed using petrophysical parameters for the evaluation of subsurface geological features and hydrocarbon potential of an onshore field in Niger Delta Basin. Four reservoir intervals were identified within the field wells based on their position within the stratigraphic column, and the reservoir correlation, which was aided using the principle of uniform horizontality, based on the simple rule that sediments are deposited horizontally and basic understanding of sequence stratigraphy. The study revealed that, the four reservoirs were predominantly sand units intercalated with shale within the reservoir units. The petrophysical evaluation revealed the Net to Gross (NTG) values ranges from 79% to 87% within the reservoir units, while the effective porosity ranges from 17% to 21%, the permeability ranges between 1307mD to 1678mD across the reservoir units, while the water saturation ranges from the lowest of 35% (reservoir C) to 78% in reservoir D. The approach validates the lithology discrimination of the elastic properties from the well logs and its effectiveness in optimizing and proper understanding of the subsurface, thus identifying and unmasking hidden features within the reservoir (probable bypass) in the field. The study has revealed that petrophysical parameters can be used quantitatively to characterize a field in terms of its lithology and fluid contents of the reservoir.

Keywords: Reservoir characterization; cross plots; discontinuity; quantitative; discrimination; stratigraphic column.

1. INTRODUCTION

Since the inception of the oil and gas industry, the need to properly explore for the natural resources using various methods has been a major priority by man, but the recent decline in the prices of oil and gas has increased exploration cost and even halted exploration activities in many oil and gas producing countries, thereby creating financial challenges to most producing and servicing companies, but the ever-increasing demands for fossil fuel energy has triggered a widespread global research for technologies, which tends to reduce the cost of exploration and improved production rate [1,2]. The desire to explore more reservoirs and deeper reserves (offshore reservoirs) has implored most oil and gas companies to embraces advance technology in their quest for more hydrocarbon. Thus, most companies will encourage the use of important tools needed for a very careful and thorough evaluation of information obtained from the subsurface. Geoscientists generally use seismic attributes in interpreting geological features especially for identifying faults and channels, in recognizing depositional environments and reveal structural deformation history. They are also useful in checking the quality of seismic data for artifacts delineation, seismic facies mapping, prospect identification, risk analysis and reservoir characterization [3]. Seismic attributes provide a link between petrophysical properties and seismic data of the reservoir, which are directly or indirectly related to rock properties of the field (Omodu et al. 2008); [4].

Real and effective estimate of facies distribution and prediction of hydrocarbon reservoir properties can be made in areas where well-log data is unavailable using the seismic patterns recognition and correlation of the data [5,6].

This research work was borne out of the fact that there is a need to reduce exploration risk and uncertainties to their barest minimum in the industry, considering the financial cost effects on exploration activities.

2. GEOLOGICAL SETTING OF NIGER DELTA

2.1 Structural Overview of Niger Delta Basin

Niger Delta basin is a large, arcuate delta of the typical, wave-and tidal-dominated type [7], which is located in the southern part of Nigeria, West Africa in the Gulf of Guinea. It is situated on the margin of West Africa shelf at the southern

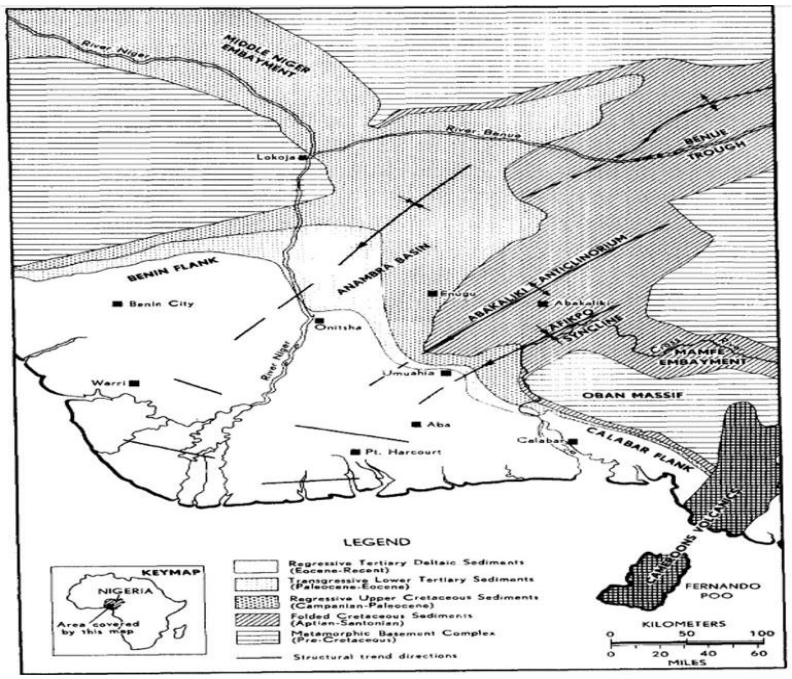

Fig. 1. Structural units of Niger Delta area [12]

culmination of the Benue trough, and it basically extends from about latitudes 4° 19′ 00″ N and 4° 50′ 00″ N and Longitudes 6° 02′ 30″ E and 7° 10′ 00″ E [8]. The delta formed at the site of a rift triple junction related to the opening of the southern Atlantic starting in the Late Jurassic and continuing into the Cretaceous as shown in Fig. 1 [9]. During the tertiary, it built out into the Atlantic Ocean at the mouth of the Niger-Benue river system, an area of catchment that encompasses more than a million square kilometers of predominantly savannah-covered lowlands [10]. The Niger Delta is a major hydrocarbon province in the world. It covers an approximate area of about 75,000 with an average thickness of about 12 km and its rank amongst the world's most prolific petroleum producing tertiary deltas that together account for about 5% of the world's oil and gas reserves [8]. The evolution of the Niger Delta is predominantly controlled by pre- and syn-sedimentary tectonics; the formations reflect a gross coarsening-upward progradational clastic wedge, which were basically deposited in marine, deltaic, and fluvial environments, as the accumulation of marine sediments in the basin probably commenced in Albian time, after the opening of the South Atlantic Ocean between the African and South American continents [11,12,13,7]. The deposition of the three formations occurred in each of the five offlapping siliciclastic sedimentation cycles that comprise the Niger Delta**,** these cycles (depobelts) are 30-60 kilometers wide, prograde southwestward, 250 kilometers over oceanic crust into the Gulf of Guinea [14].

2.2 Chronostratigraphy

The Niger Delta basin consists of Cretaceous to Holocene marine clastic strata that overlie

oceanic and fragments of continental crust (Fig. 2) [15,16]. They also stated that the Cretaceous section has not been penetrated beneath the Niger Delta basin, and thus, Cretaceous lithologies can only be extrapolated from the exposed sections in the next basin to the northeast around the Anambra basin. In this basin, Cretaceous marine clastic consist mainly of Albian–Maastrichtian shallow-marine clastic deposits [17,18], while on the other hand, the Tertiary Niger Delta represents a succession of alternating deep-water, shallow marine, and deltaic sands and shales that began prograding onto a passive continental margin as early as Eocene time [16]. Sediments has been transported to the delta through the Benue Trough/Bida Basin failed rift system where the total Tertiary section may reach up to 12 km in thickness near the center of the basin [7].

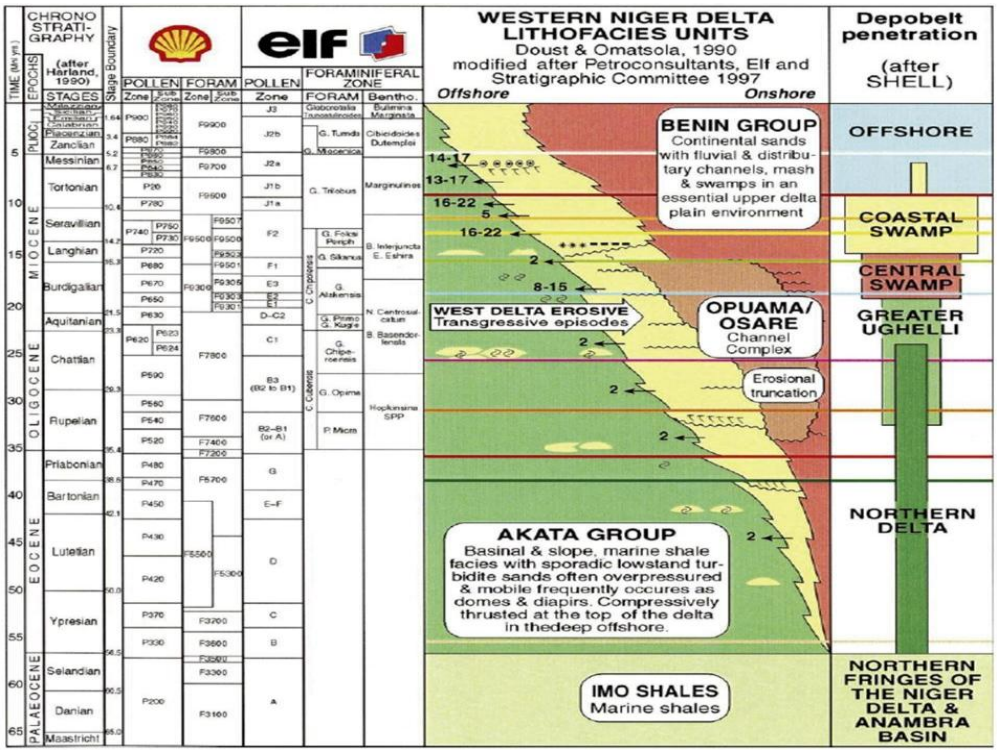

Fig. 2. Regional stratigraphy of Western Niger Delta [15]

2.3 Depobelts

The deposition of the three major formations occurred in each of the five offlapping siliciclastic sedimentation cycles that comprise the Niger Delta**, t**hese cycles (depobelts) are 30-60 kilometers wide, prograde southwestward, 250 kilometers over oceanic crust into the Gulf of Guinea [14]. They are well defined by syn-sedimentary faulting that occurred in response to variable rates of subsidence and sediment supply with each depobelt as a separate unit that corresponds to a break in the regional dip of the delta and is bounded landward by growth faults and towards the sea by large counter-regional faults or the growth fault of the next seaward belt [7]. Five major depobelts are generally recognized which include the Northern, Greater Ughelli, Central Swamp, Coastal Swamp and Offshore depobelts (Fig. 3), each with its own sedimentation, deformation, and petroleum history [7,19,20].

2.4 Location of Study Area

The study area is located within the onshore area of Niger Delta basin in Nigeria, known as A-Field (Fig. 3). The terrain is generally swampy in nature, with river channels and tributaries emptying into the Atlantic Ocean. The Field lies between longitude 6°17"55'E and latitude 4°37"27'N, located within the Central Swamp Depobelt, Onshore Niger Delta.

3. THEORETICAL BACKGROUND

3.1 Well Logs

A well log is a record of measurements of the subsurface formation properties in a well, they

are routinely used for stratigraphic interpretation of the earth's subsurface; Well logs are detailed record of the geologic formations penetrated by a borehole, and are physical measurements made by lowering of specialized instruments into the hole. Logging of a well can be done during completion, producing or abandoning which is performed in boreholes drilled for oil and gas, groundwater, mineral, and geothermal exploration, as well as part of environmental and geotechnical studies. Well logs are generally prepared in order to evaluate hydrocarbon deposits and some of these logs include gamma ray, sonic, resistivity (deep, medium & shallow), neutron-porosity, density and caliper [21].

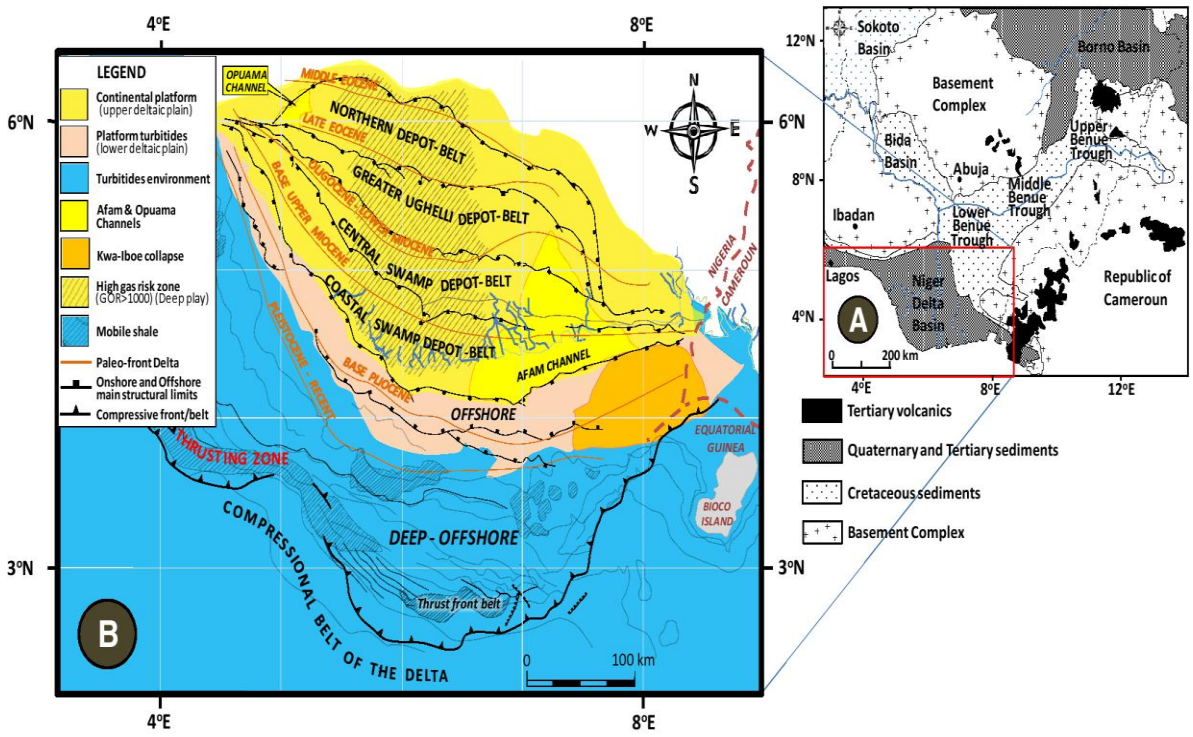

Fig. 3. Geologic map of Nigeria showing the location of the Niger Delta Basin and sectional map of the Niger Delta depobelts and structural limits [7]

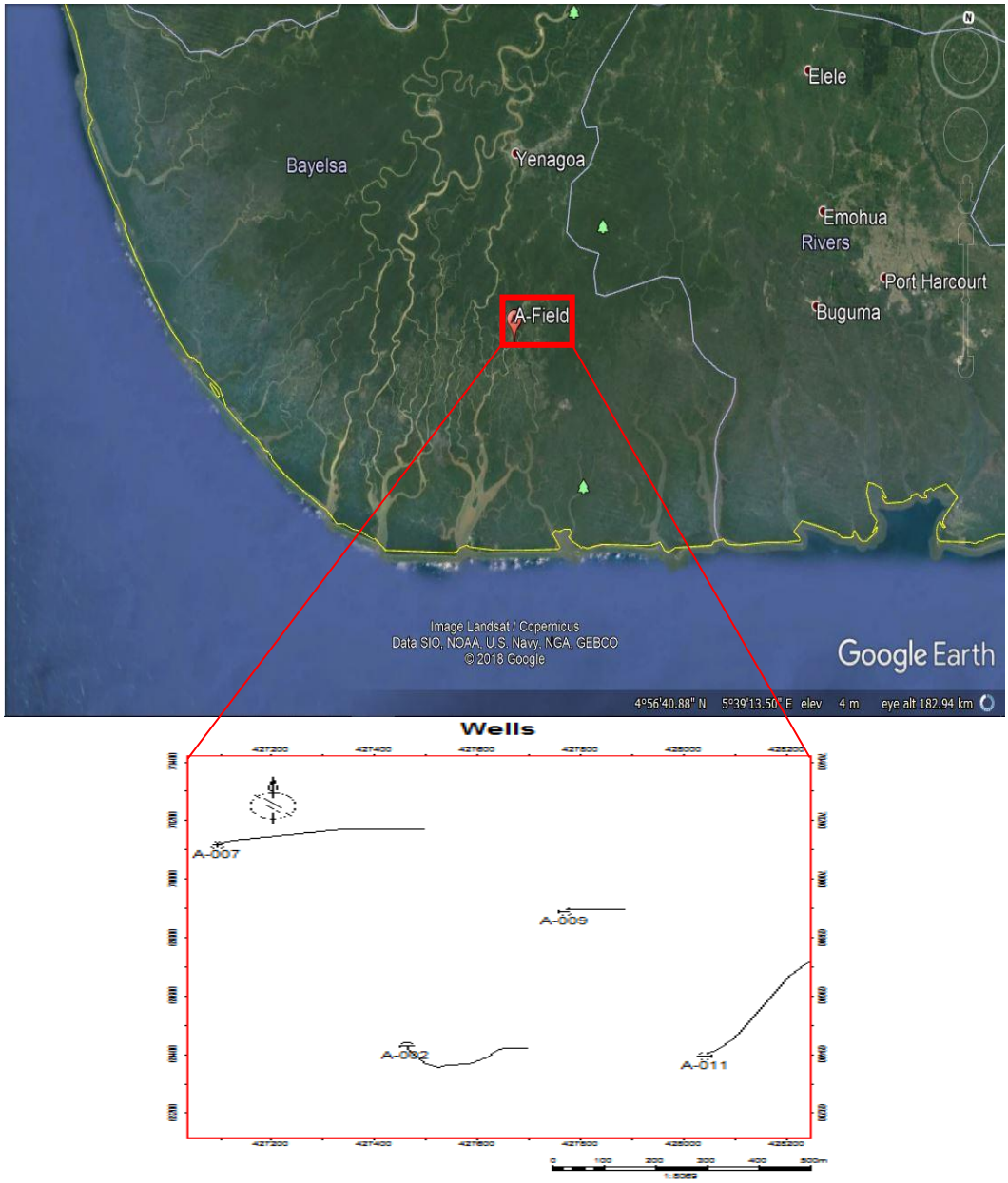

Fig. 4. A map showing the location of the A-Field, Central Swamp Depobelt, Onshore Niger Delta (Source: Google Earth 2018) and the Base map for A-Field showing the distribution of wells within the area

3.2 Types of Well Logs

3.2.1 Gamma ray logs

This is the measurement of the natural radioactivity in a formation or response to the presence of uranium, potassium- and thorium-rich minerals in the formation. As the clay content increases, the gamma ray response increases; organic-rich marine shale commonly has the greatest response as it contains significant amounts of uranium-rich minerals generated by the reduction of decaying organic matter [21]. The GR is used primarily to define the volume of shale (*V*sh) in a sequence, especially where the self-potential (SP) response is distorted or where oil-based mud is being used [22]. When comparing GR logs from a number of wells, they should all be normalized to a common scale, as each tool will have been calibrated individually. This is especially true if being used for correlation or quantitative calculations.

3.2.2 Porosity logs

This measures the ratio of the volume of pore (void) space (*V*p) to the total volume of rock (*V*t), which can be described as primary or secondary porosities depending on whether mineral dissolution has occurred during lithification [21,22]. Porosity can also be classified as either total (PhiT) or effective (PhiE), depending on the source of the measurement; core data are generally assumed to be 'total' because of the cleaning and drying process in the laboratory, but a log-derived measurement could be either effective or total depending on how it has been derived. A number of logs measure porosity, although none actually does this directly, three common tools exist namely the sonic log, which measures the acoustic response of a formation while the density and neutron logs takes nuclear measurements. When these tool responses are combined, two or three at a time, lithology can also be determined, along with a representative porosity interpretation [21].

3.2.3 Sonic log

The sonic log measures the interval transit time of a compressional sound wave traveling through the formation along the axis of the borehole wall, a compressional sound wave can travel in solids, liquids and gases; however, the fastest path for the wave to follow is through the solid (Schlumberger, 1989). The interval transit time (Δ*t*) is the reciprocal of the velocity of the sound wave passing through the formation and is measured in microseconds per foot or metre (µs/m or µs/m). Sonic logs can be mathematically derived from:

$$\emptyset_{Sonic} = \frac{\Delta t \log - \Delta tma}{\Delta t_f - \Delta tma} \times \frac{1}{C_p} \quad (1)$$

ϕ_{Sonic} = Sonic derived porosity
Δt_{ma} = interval transit time of matrix (given)
Δt_{log} = Interval transit time of formation
Δt_F = Interval transit time of fluid in the well bore (Fresh mud = 189, salty mud = 185)

$$C_p = \frac{\Delta t_{sh} \times c}{100} \quad (2)$$

C_p = compaction factor
Δt_{sh} = Interval transit time of adjacent shale
C = a constant, normally 1.0 (Hilchie, 1978).

3.2.4 Density logs

The density log measures the bulk density of the formation; that is, the density of the rock plus the fluids contained in the pores. Density is measured in g/cm^3 and is by convention given the symbol ρ (rho) [21,22]. Porosity value can be estimated using the density tool, it is necessary to know the matrix density and the density of any fluids in the pore space. Porosity from the density log is calculated using the equation.

$$\emptyset_{Den} = \frac{\rho ma - \rho_h}{\rho ma - \rho_f} \quad (3)$$

ϕ_{Den} = Apparent density porosity
ρ_{ma} = Matrix density
ρ_b = Bulk density log reading
ρ_f = Fluid density (1.1 salt mud, 1.0 fresh mud and 0.7 gas)

3.2.5 Neuron log

Neutron logs measure the hydrogen concentration in a formation, the hydrogen index (HI) from its commonest source of hydrogen in the formation which are water or hydrocarbons. In shale-free rocks where the pore space is filled with water or oil, the neutron log directly measures liquid-filled porosity and where the pores are filled with gas the concentration of hydrogen is reduced, resulting in a lower porosity reading from the tool, which is called the gas effect [22]. The neutron porosity is calculated directly from the log response, as the tool measures liquid-filled porosity; it is usually calibrated in limestone porosity units and must, therefore, be corrected for the actual lithology. The relationship between the neutron count rate and porosity can be expressed mathematically as

$$\log_{10} \emptyset = aN + B \quad (4)$$

a = constant
B = constant
N = count rate and ϕ is the true porosity.

3.2.6 Resistivity Logs

This is used to measure the subsurface electrical resistivity which helps to differentiate between formations filled with salty waters (good conductors of electricity) and those filled with hydrocarbons (poor conductors of electricity). Resistivity log measurement is very important in the determination of hydrocarbon and when combined with porosity logs, they can be used to calculate hydrocarbon saturation and to delineate

potential reservoirs [23]. The resistivity of the formation depends on the pore geometry, fluid present in the formations with a high possibility of obtaining hydrocarbon but lower readings show the presence of water due to its conductivity, it is expressed in ohms. Resistivity logs includes Micro-logs normal/inverse, Micro-Laterolog, Proximity log, Micro-Spherically Focused log, Laterolog, and Induction log [21].

3.3 Petrophysical Properties

Petrophysics is a study of the physical and chemical properties of rock and their interactions with fluids. It is majorly applied in the study of reservoirs for the hydrocarbon industry and some of the key properties studied are Gross and Net thickness, porosity, fluid saturation, permeability, Net to Gross ration and shale volume. An important aspect of petrophysics evaluation is the measurement and evaluation of rock properties by acquiring well log measurements. The major petrophysical properties obtained from well log measurements are as follows:

3.3.1 Gross and net thickness

The gross thickness of the reservoir is the entire thickness of the reservoir, including the shaly sections of the reservoir while the net sand is the interval of sand in the reservoir that is clean, containing no shaly fractions. The net sand thickness is computed after the volume of shale within the reservoir has been determined and the thickness value subtracted from the total reservoir thickness.

3.3.2 Porosity

Porosity may be defined as *effective* or *total* depending on whether it includes porosity associated with clays; some tools measure total porosity and must be corrected for the clay content.

Total porosity (Φ_T) and effective porosity (Φ_E) are calculated using Wyllie's equation as follows;

$$\emptyset_T = \frac{\rho_{ma} - \rho_{bulk}}{\rho_{ma} - \rho_{fl}} \quad (5)$$

$$\emptyset_E = \emptyset_T - (\emptyset t_{sh} \times Vsh) \quad (6)$$

Where;

Φ_T = density derived porosity
ρ_{ma} = matrix density taken as 2.65g/cm^3
ρ_{bulk} = matrix density taken as bulk density log values
ρ_{fl} = fluid density taken as 1.00g/cm^3
V_{sh} = Shale volume
Φ_{tsh} = Total porosity of shale

3.3.3 Fluid saturation

Fluid saturation in petrophysics comprises of both water and hydrocarbon saturation contents. Water saturation (*S*w) is the proportion of total pore volume occupied by formation water; for water saturation (Sw), from Archie's [24] empirical equation was utilized as follows;

$$\text{Sw} = \left(\frac{a \times R_w}{R_t \times \emptyset_t^m}\right)^{1/n} \quad (7)$$

Where;

S_{wa} = Archie's water saturation for clean sand
a = Tortuosity factor that is 1
m = Cementation exponent which is 2
n = Saturation exponent that is 2
Rt = Formation resistivity (read from log)
Rw = Formation water resistivity (read from log)
Φ_t = Total Porosity

Hydrocarbon saturation is the proportion of fluid that is (oil and gas) and is derived from the relationship

$$S_H = 1 - S_w. \quad (8)$$

3.3.4 Permeability

Permeability (*k*) is the measurement of the capacity of a reservoir to conduct fluids or its ability to allow flow to take place between the reservoir and a wellbore; which also dependent on the associated rocks and fluid properties. Permeability occur as effective permeability (K_{eff}), which is the permeability of one liquid phase to flow in the presence of another; relative permeability (*K*r), the ratio of effective to absolute permeability for a given saturation of the flowing liquid (i.e. permeability of oil in the presence of water (K_{ro})) and absolute permeability. Permeability is measured in Darcies (D) and can be calculated using the equation given as [25]:

$$K(mD) = 307 + 26552\,(\emptyset^2) - (\emptyset \times S_w)^2 \quad (9)$$

3.3.5 Net-To-Gross (NTG)

This is the total amount of pay footage divided by the total thickness of the reservoir. It can be calculated as the oil initially in place (OIIP) or Gas initially in place (GIIP), assuming that the entire reservoir interval is used to determine the

total volume of hydrocarbons present within the reservoir interval. Net-To-Gross is a measure of the potential of the productive part of a reservoir. It is usually expressed either as a percentage or fraction of the producible (net) reservoir within the overall (gross) reservoir packages [26-32]. The higher the Net to Gross, the better the reservoir quality and it is expressed as:

$$\text{Net-to-gross} = \frac{NT}{GT} \times 100 \quad (10)$$

NT = Net thickness
GT = Gross Thickness

3.3.6 Shale volume

This is the space occupied by shale or the fraction of shale (clay) present in reservoir rocks, the volume of shale in a reservoir plays a key role in hydrocarbon production where the higher the reservoir shaliness, the poorer the reservoir productivity [27-35]. The magnitude of the gamma ray count in a formation of interest is related to the shale content of the formation and the relationship may be linear or non-linear. Shale volume is often calculated using Larionov's equation [26, 36- 42] for tertiary sands as follows;

$$Vsh = 0.083 * (2^{(3.7 * GR_{index})} - 1 \quad (11)$$

Where

$$GR\log = GR\log reading$$
$$GR\min = GR\ sand\ baseline$$
$$GR\max = GR\ shale\ baseline$$

4. METHODOLOGY

4.1 Materials and Methods

This study was conducted using well log data obtained (recorded) from the onshore field (A-Field) of Niger Delta Area. Some of the available data are the well log suite, which comprises of Gamma ray (GR) logs, Caliper logs, Porosity logs (neutron, density and sonic) and resistivity (shallow and deep) with their well header information, check shot data and well survey deviation data. Two major industrial softwares were used for the processing and interpretation.

4.1.1 Research design and workflow

The following outlined workflow was utilized for the study as shown in Fig. 5:

1. Data sourcing, data gathering, and data loading into relevant software.
2. Data quality assurance and quality control.
3. Well logs conditioning (despiking and interpolation).
4. Well correlation.
5. Petrophysical evaluation of reservoirs.
6. Attribute cross plots from well logs
7. Hydrocarbon Prospect evaluation
8. Volumetric evaluation.

4.1.2 Methods

The data set were quality checked and sorted into acceptable format for the software namely: Petrel™ software which was used for data appraisal, well correlation, petrophysical analysis and evaluation, as well as generation of hydrocarbon prospect while the Hampson Russell software was used for lithology evaluation and fluid discrimination respectively.

Prior to loading the data into the respective softwares, the project geographic reference zone, coordinates, and units were determined and set. The well header information was uploaded; this contains the names of all the wells, their geographic references, the total drilled depth and also the well reference datum. A total of 4 wells were available and utilized for this study which included; Well A-002, A-007, A-009, and A-011 as shown on the base map (Fig. 4), the wells distributions were not even across the area. The well deviation, which defines the trajectory of the well, shows the heterogeneity of geologic layers.

Well logs were available, Gamma Ray log in gAPI unit, Deep Resistivity in Ohm.m, Density in g/cm^3, Neutron in m^3/m^3 and Sonic in µs/m. All well log depths were available in feet.

Table 1. Well data inventory for four wells utilized in this study

Well Name	Well logs						Well Header	Check shot	Directional Survey
	GR	Cali	Res	Den	Neutron	Sonic			

A-002	YES	YES	YES	YES	YES	YES	YES	NO	YES
A-007	YES	YES	YES	YES	YES	YES	YES	NO	YES
A-009	YES	YES	YES	YES	YES	YES	YES	NO	YES
A-011	YES	YES	YES	YES	YES	YES	YES	YES	YES

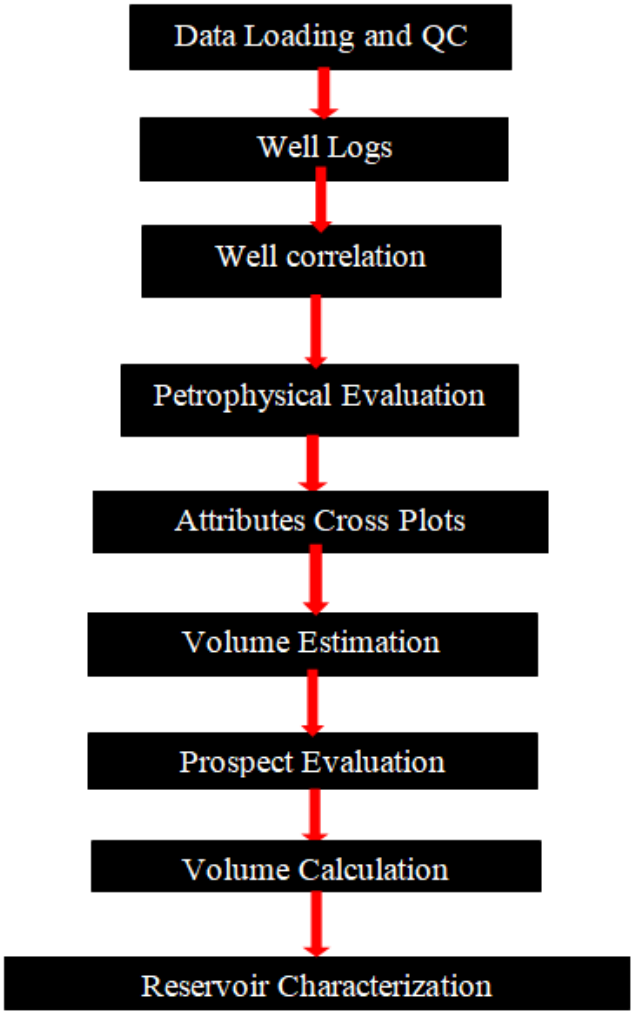

Fig. 5. Workflow utilized for the analysis of A-Field

The Gamma ray log differentiated the lithology into sand and shale, high resistivity log readings identified sand zones for hydrocarbon accumulation and low resistivity readings indicated shale zone. A cross plots of neutron and density logs were performed to characterize the fluid content in the reservoir in order to indicate areas of hydrocarbon.

Checkshot data provided was for well A-011 only, which was loaded and displayed in a function window for conditioning by displaying as a graph with depth on the vertical axis and TWT on the horizontal axis to check for any spikes not related to geology. There was no spike (outlier), hence the checkshot was of good quality.

4.1.3 Well logs correlation

Correlation was done between the wells to identify specific reservoir formations encountered within the different wells; the well correlation identification was achieved using the gamma ray log measurements. The GR scale was set from 0 to 150 gAPI on the GR tract, based on the defined cut-off, GR deflections to the right of the cut-off classified as clean sand while deflections to the left of the tract are classified as shales. Three stacking patterns identified from the correlation and identification of depositional environment in the field includes; progradational

(bell-shaped), retrogradational (funnel-shaped) and aggradational (blocky).

4.1.4 Fluid contact delineation

The oil water contact (OWC) was determined with the aid of the resistivity log based on the fact that oil is more resistive than brine; there was a sharp rise in resistivity, which is an indication of the presence of hydrocarbons in the reservoir. Meanwhile, neutron and density logs were used to ascertain the type of hydrocarbon presence in the reservoirs. Oil zones were majorly identified due to the effect of the cross over between neutron and density logs which showed a small separation.

4.1.5 Petrophysical properties estimation

The petrophysical parameters for the reservoir zones in the different wells were calculated using the relevant equations given above. The following petrophysical parameters were estimated namely; fluid saturation (water and hydrocarbon saturation), shale volume, permeability, porosity (total and effective), these values were plotted in the log sections.

4.1.6 Extracted attributes cross plots analysis

In order to delineate the extent and determine the volume of hydrocarbon in-place in probable reservoirs identified interval in the wells, some of the extracted attributes from the well logs are estimated and cross plotted (using 3-D cross plots), where the 3rd dimension connotes the colour coding of the data points using Hampson-Russell software. Three major attributes of the well data estimated and used to delineate the lithology as well as discriminates fluid contents in the reservoir, are basically the two lame's parameters (elastic moduli), namely Lambda-rho (incompressibility modulus - λρ) and Mu-rho (rigidity modulus - μρ) and the acoustic impedance.

$$\text{Lambda-Rho } (\lambda\rho) = (\text{P-impedance})^2 - C \times (\text{S-impedance})^2 \quad (12)$$

$$\text{Mui-Rho } (\mu\rho) = (\text{S-impedance})^2 \quad (13)$$

$$\text{P-impedance} = \text{P-wave} \times \text{Density} \quad (14)$$

5. RESULTS AND DISCUSSION

The results obtained from the study, which includes results from the well log evaluation of the selected wells, delineation of the well lithology, correlation of the wells, petrophysical analysis and evaluation of the properties and cross-plot analysis for computing the attributes for fluid discrimination are presented in the following Figs. 6-12. The results of this study are presented in the following order; well log evaluation of the selected wells, well correlation, petrophysical parameter analysis, cross plot for attributes computed to identify lithology and fluid discrimination, and volumetric estimation. These obtained reservoirs parameters were used for petrophysical evaluation of the reservoir properties, namely Shale Volume, Effective porosity, Permeability, Hydrocarbon and water saturation as shown in the Figs. 8-11, while the estimated values are tabulated in Table 1. The fluid contents in the reservoir sand units were discrimination using the resistivity log and the cross plot analysis.

5.1 Well Log Evaluation

Based on the gamma ray logs, two lithologies were identified; sand and shale. From the gamma ray log, the interval coloured yellow is identified as sand due to low value in gamma ray, while the gray-yellow for shale is as a result of high gamma ray readings. The gamma log signatures indicate areas with sand and shale. The resistivity log signatures indicate a higher value at a point where the gamma ray logs reading is low (a probable sand interval), while the high resistivity signature is indicative of brine sand. The cross plot of density and neutron log signatures conform to the gamma ray log readings indicating oil and water zones in the reservoir (the reservoir consist mainly of oil and water with little or no gas present).

5.2 Well Correlation

Four lithological reservoirs were identified from the results of the correlation as the reservoirs of interest for this study, Reservoir A (A-002), B (A-007), C (A-009), and D (A-011) based on gross thickness and presence of significant pay thickness with reservoir tops ranging from 3288.84m to 3698.26m for well A-002, 3279.63m to 3495.56m for well A-007, 3324.77m to 3542.24m for well A-009 and 3318.15m to 3530.90m for well A-011 respectively, while the reservoir base depths were taken at 3357.86m to 3698.26m for well A-002, 3352.23m to 3683.57m for well A-007, 3389.06m to 3660.44m for well A-009, and 3384.34m to 3720.01m for A-011 respectively as shown in Fig. 6a-d.

5.3 Results of Petrophysical Analysis

The results of the petrophysical evaluation estimated for the identified reservoirs in A-field are presented in Table 2, while Fig. 7 shows the petrophysical logs derived from the available conventional well logs.

5.4 Gross Thickness

The gross thickness of a reservoir as shown in Fig. 7, is the thickness of the reservoir interval (from the top of the reservoir to the base of the reservoir). From the results, the thickness varies from one well to the other across the field. The thickness of reservoir A is 69m in well A-002, 72m in A-007, 64m in A-009 and 66m in well A-011 (Table 2). Reservoir B has a thickness of 29m in well A-002, 26m in A-007, 26m in A-009 and 14m in well A-011. The thickness of reservoir C is 16m in well A-002, 29m in A-007, 29m in well A-009 and 23m in well A-011 and reservoir D is 177m in well A-002, 188m in A-007, 118m in well A-009 and 189m in well A-011. On average, the gross thicknesses of the reservoirs are: reservoir A is 67.75m, reservoir B is 23.75m, reservoir C24.25m and 168m for reservoir D respectively. From the results we can conclude that reservoir D has the highest average thickness and reservoir B with the least average thickness. These results show that the various reservoir sands are of sufficient thickness in accumulating hydrocarbons in economic quantities.

5.5 Shale Volume (Vsh)

Shale volume is the percentage of shale contained within the reservoir. The higher the percentage of the shale contents in the reservoir, the poorer the reservoir quality to yield hydrocarbons. In reservoir A, shale volume ranges from 14-30% across the four wells and accounts for a thickness of 9.66m of the entire gross thickness in A-002 well, 12.24m in A-007 well, 14.72m in A-007 well and 19.8m in A-011 well (Table 2), while in reservoir B, shale volume ranges from 12-15% in the wells. Quantifying the shale volume in terms of thickness shows that 3.48m, 3.64m, 3.38m, and 2.1m are the

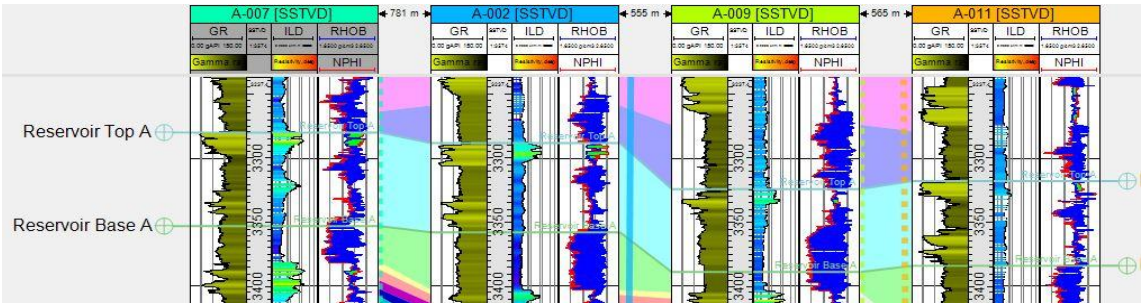

Fig. 6a. Identification and correlation of reservoir A

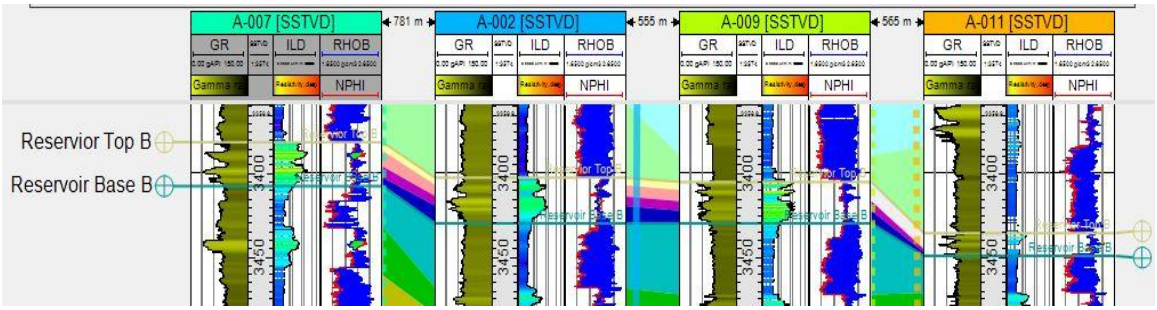

Fig. 6b. Identification and correlation of reservoir B

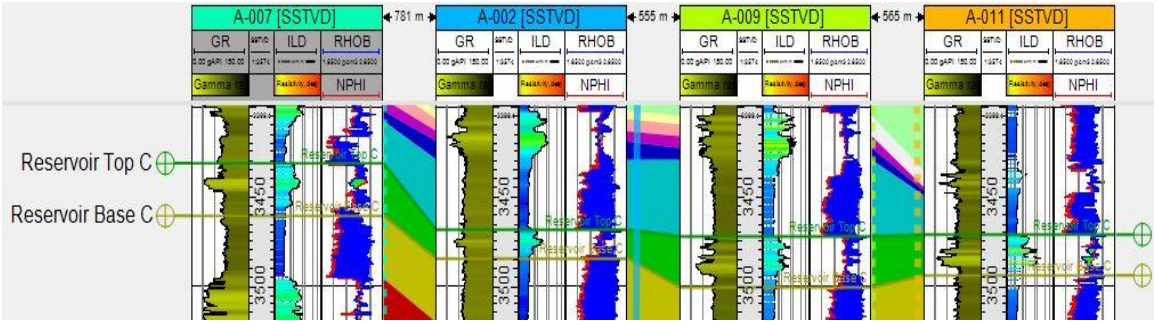

Fig. 6c. Identification and correlation of reservoir C

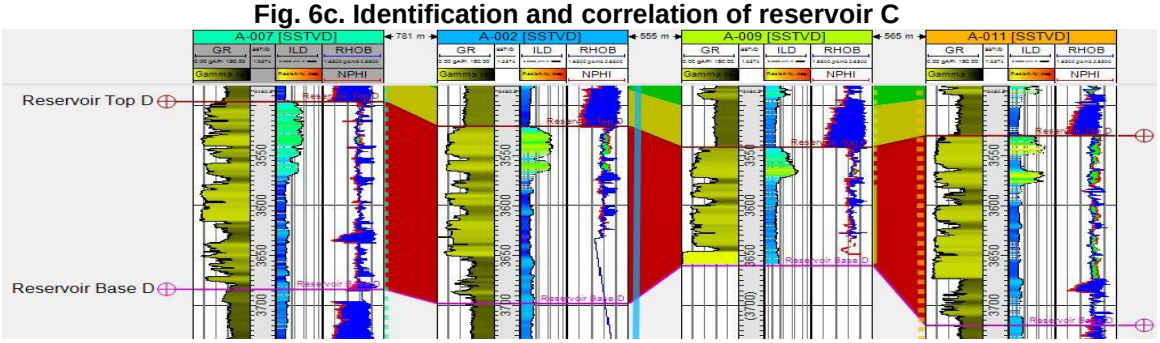

Fig. 6d. Identification and correlation of reservoir D

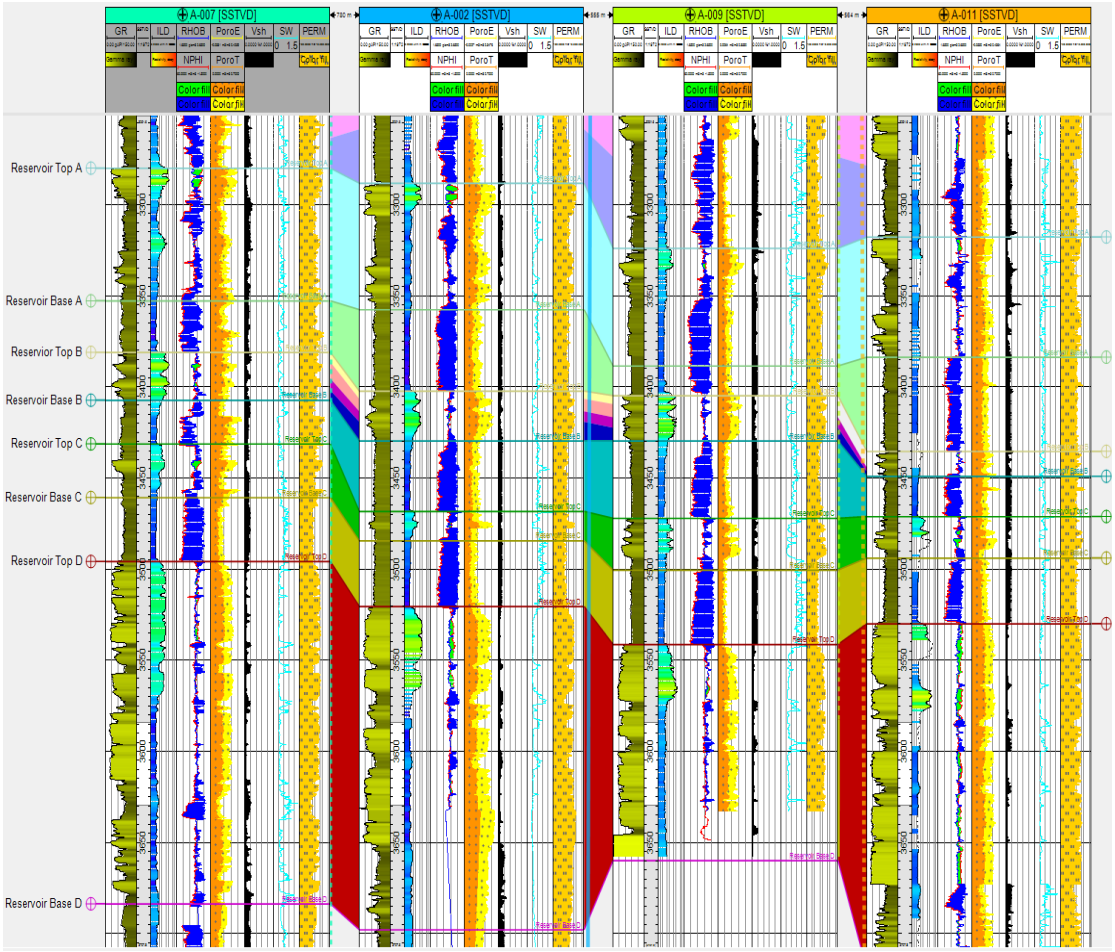

Fig. 7. The Correlated wells showing the estimated petrophysical parameters

thicknesses of shales in reservoir B in the wells respectively (Table 2). The shale volume in reservoir C ranges from 12-14% across the well, which translates to a thickness of 23.01m, 3.77m, 4.06m and 3.22m in A-002, A-007, A-009, and A-011 respectively and for reservoir D, the values ranges from 13-16% across the wells, which translates to a thickness of 23.01m, 26.32m, 15.34m and 30.24m in A-002, A-007, A-009, and A-011. On average, shale volume thickness is 14.11m in reservoir A, 3.15m in reservoir B, 3.24m in reservoir C, and 23.73m in reservoir D (Fig. 8). This suggests that about 14.11m of the average gross thickness in reservoir A is occupied by shale, while reservoir B is occupied with an average thickness of 3.15m shale, Reservoir C is occupied by an average shale thickness of 3.24m while 23.73m of the average gross thickness of reservoir D is shale.

Table 2. Results of petrophysical evaluation of three reservoir units for four wells in the a-field

Wells	Reservoir sands	Top (m)	Base (m)	Gross thickness (m)	Shale volume (%)	Shale volume (m)	Net sand (m)	Net-to Gross (%)	Total Porosity (%)	Effective Porosity (%)	Water saturation (%)	Permeability (mD)	Hydrocarbon saturation (%)	Fluid type
Well 002	A	3289	3358	69	14%	9.66	59.34	86%	22%	20%	59%	1744.303	41%	Oil/water
	B	3402	3431	29	12%	3.48	25.52	88%	19%	17%	56%	1155.55	44%	Oil/water
	C	3469	3485	16	12%	1.92	14.08	88%	13%	11%	82%	691.9105	18%	Oil/Water
	D	3521	3698	177	13%	23.01	153.99	87%	20%	19%	78%	1636.715	22%	Oil/Water
Well 007	A	3280	3352	72	17%	12.24	59.76	83%	24%	22%	42%	1540.439	58%	**Oil**
	B	3381	3407	26	14%	3.64	22.36	86%	25%	21%	52%	1821.868	48%	**Oil/Water**
	C	3431	3460	29	13%	3.77	25.23	87%	28%	25%	41%	2019.133	59%	**Oil**
	D	3496	3684	188	14%	26.32	161.68	86%	26%	22%	82%	2214.002	18%	**Oil/Water**
Well 009	A	3325	3389	64	23%	14.72	49.28	77%	25%	23%	35%	2037.376	65%	**Oil**
	B	3404	3430	26	13%	3.38	22.62	87%	19%	17%	66%	1254.444	34%	**Oil/Water**
	C	3472	3501	29	14%	4.06	24.94	86%	15%	14%	56%	1001.586	28%	**Oil/Water**
	D	3542	3660	118	13%	15.34	102.66	87%	15%	14%	76%	995.2449	24%	**Oil/Water**
Well 011	A	3318	3384	66	30%	19.8	46.2	70%	19%	16%	78%	1313.773	22%	**Oil/Water**
	B	3435	3449	14	15%	2.1	11.9	85%	19%	16%	51%	991.2469	49%	**Oil/Water**
	C	3471	3494	23	14%	3.22	19.78	86%	29%	24%	44%	2276.725	56%	**Oil**
	D	3531	3720	189	16%	30.24	158.76	84%	19%	17%	81%	1434.346	19%	**Oil/Water**

5.6 Net Thickness

The reservoir net thickness is the proportion of the reservoir (clean sand) that can be produced. The difference in thickness of the overall gross volume and the shale volume give the net reservoir thickness. The net sand thickness of reservoir A is 59.34m in A-002 well, 59.76m in A-007, 1661.68m in A-009 and 46.2m in A-011 well (Table 2). In reservoir B, the net sand thickness is 25.52m in A-002 well, 22.36m in A-007, 22.62m in A-009 and 11.9m in A-011 well respectively. Similarly, reservoir C has a net sand thickness of 14.08m, 22.36m, 24.94m and 19.78m in A-002, A-007, A-007, and A-011 wells then reservoir D has a net sand thickness of 153.99m, 161.68m, 102.66m and 158.76m in A-002, A-007, A-007, and A-011 wells respectively. The average net sand (clean sand) thickness for reservoir A is 53.65m, 20.6m for reservoir B, 21.01m for reservoir C and 144.27m for reservoir D (Fig. 6).

5.7 Net-To-Gross

The ratio of the thickness of the clean sand (net sand thickness) to the total gross thickness of the reservoir gives the net to gross value. The net to gross gives the total amount of the reservoir section that can be produced, thus the larger the net to gross value, the better the quality of the reservoir producible. The net to gross value for reservoir A, ranges from 70-86% across the wells (Table 2), while for reservoir B, the value of net to gross ratio ranges from about 85-88% in the wells. Similarly, for reservoir C, the net to gross ratio ranges from 86-88% across the wells and for reservoir D, the value falls between a net to gross of 84-87% in the wells. The average net to gross ratio for reservoir A, B, C, and D ranges from 79-86.75% respectively (Table 2), this results show that on average, over 84.56% of the entire gross thickness of the reservoirs can be produced if they contain hydrocarbons.

5.8 Porosity

The total sum of the interconnected pores and the isolated pore spaces gives the total porosity values (Fig. 9). The porosity relevant for hydrocarbon production is the effective porosity, thus the effective porosity is defined as the sum of all the interconnected pore throats in the reservoir. In this study, the result of total porosity for reservoir A is 22% in A-002 well, 24% in A-007, 25% in A-009 and 19% in A-011 well (Table 2), while the effective porosity is 20%, 22%, 23% and 16% in respectively in the wells (A-002, A-007, A-009 and A-011). For reservoir B, total porosity are 19%, 25%, 19% and 19% respectively, while the effective porosity are 17% for A-002, 21% for A-007, 17% for A-009 and 16% for well A-011. Similarly, for reservoir C, total porosity is 13%, 28%, 15% and 29% while effective porosity is 11%, 25%, 14% and 24% for A-002, A-007, A-009 and A-011 wells and for reservoir D, total and effective porosity are 20% and 19% for well A-002, 26% and 22% for A-007, 15% and 14% for A-009 and 19% and 17% for well A-011 respectively. The average porosity for reservoir A, both total and effective are 22.5% and 20.25%, while for reservoir B the values are 18% and 17.75% for reservoir B. reservoir C has values of 21.25% and 18.5% and reservoir D has 20% and 18%, respectively (Fig. 9). According to Rider classification (1986), porosity measurements <5% are considered negligible, between 5-10% are poor, >10-20% are good, >20-30% are very good and >30 are excellent. Based on this classification scheme which is globally accepted for porosity classification, the total porosity recorded from reservoirs B and D are classed as good, while reservoirs A and C are classified as very good while effective porosity recorded for reservoir A, B, C and D are classed as good.

5.9 Permeability

The ability of fluids to seamlessly flow through any reservoir rock is referred to as the permeability of the reservoir, Fig. 10 shows the permeability measurements calculated in this study. The results of permeability for reservoir A is 1744.303mD in A-002 well, 1540.439mD in A-007, 2019.133mD in A-009 and 1313.773mD in A-011 well (Table 2). For reservoir B, permeability is 1155.55mD, 1821.868mD, 1254.444mD and 991.2469mD in A-002, A-007, A-009, and A-011 wells respectively. The permeability values calculated for reservoir C, are 691.9105mD, 2019.133mD, 1001.586mD and 2276.725mD in A-002, A-007, A-009, and A-011 wells, while for reservoir D, the values are 1636mD, 2214mD, 996mD, and 1434mD respectively. On average, permeability values calculated are 1658.9728mD, 1305.7772mD, 1497.338625mD, and 1570.0770mD in reservoirs A, B, C and D respectively (Fig. 10). Using Rider (1986) permeability values classification principle, the reservoir quality are classified as follows; < 10mD (poor to fair), >10-50 mD (moderate), >50-250 mD (Good), >250-1000 mD (very good) and >1000 mD (excellent). Using this classification principle, reservoir A, reservoir B, reservoir C and reservoir D can be

classed as very good to excellent reservoirs because they have average permeability values ranges >1000mD. These results show that all the reservoirs in the field have very good to excellent permeability values which are necessary requirements for hydrocarbon flow and production in economic quantities.

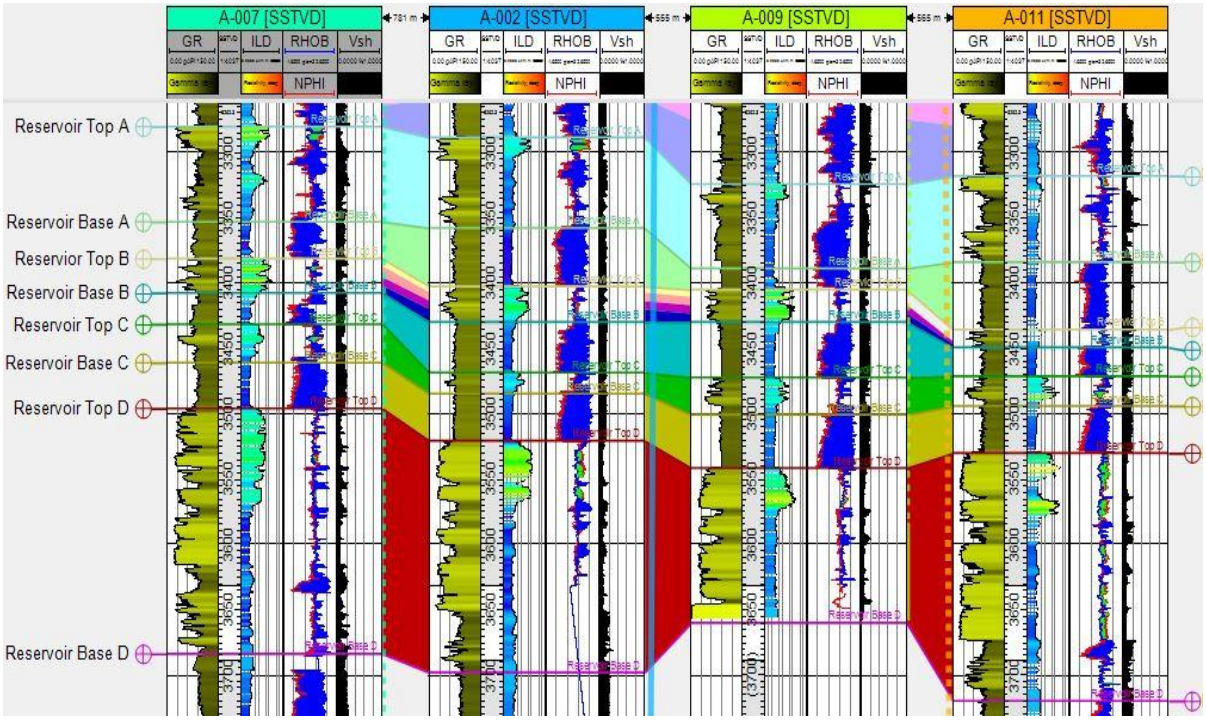

Fig. 8. Shale volume values calculated for the four reservoir intervals and correlated across all four wells

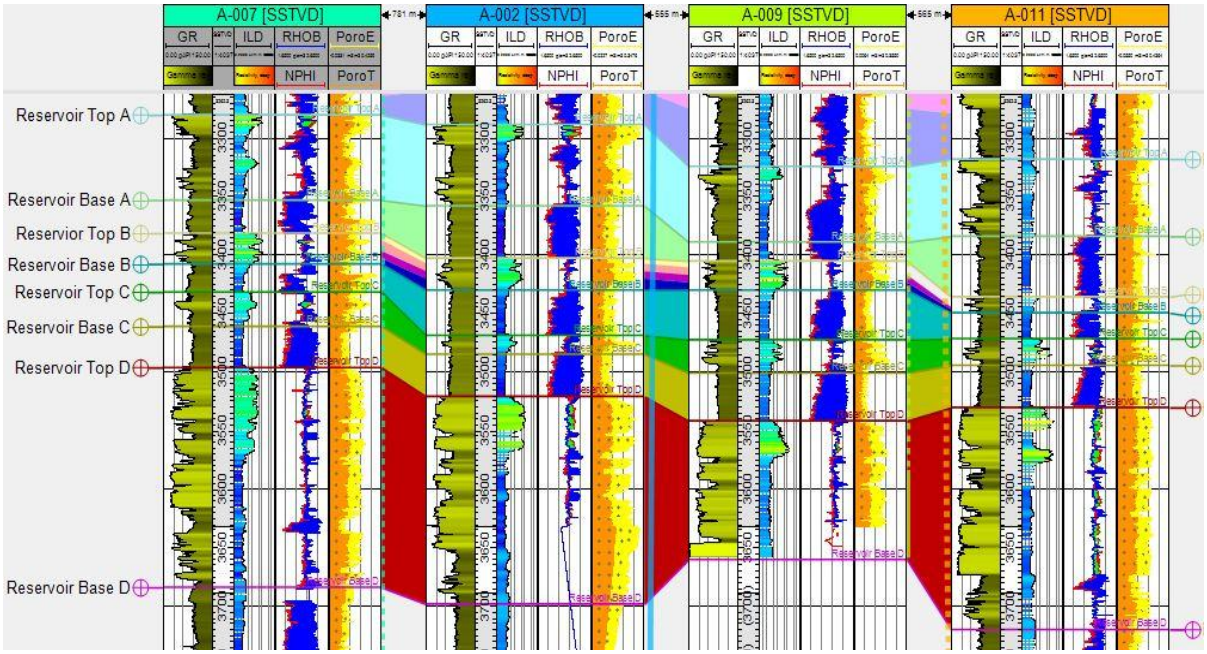

Fig. 9. Porosity values calculated for the four reservoir intervals and correlated across all four wells

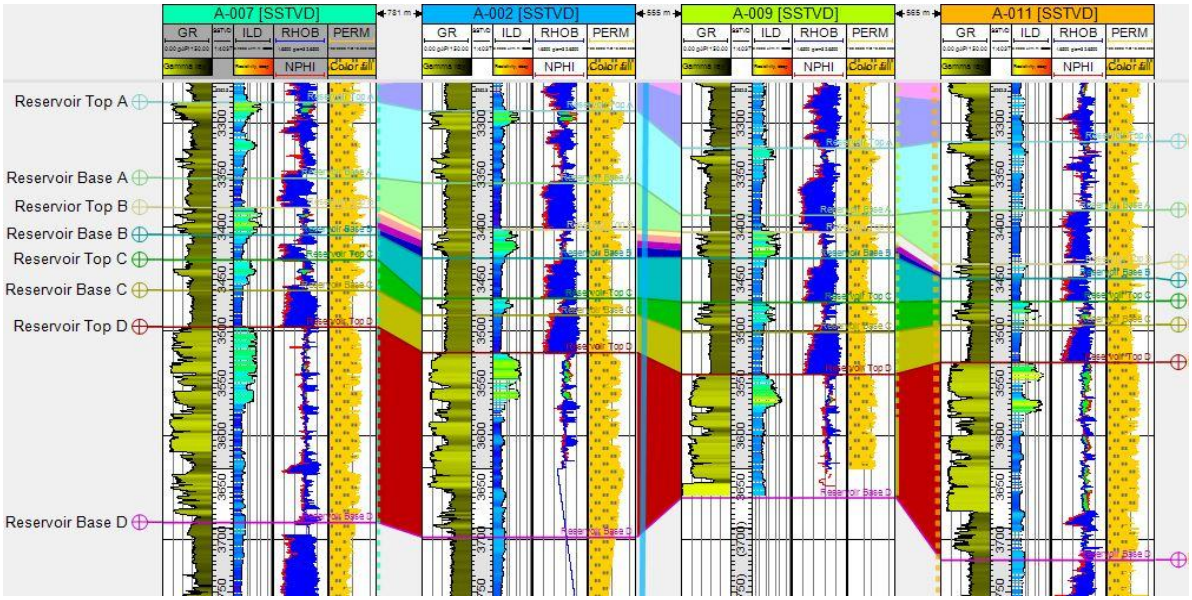

Fig. 10. Permeability values calculated for the four reservoir intervals and correlated across all four wells

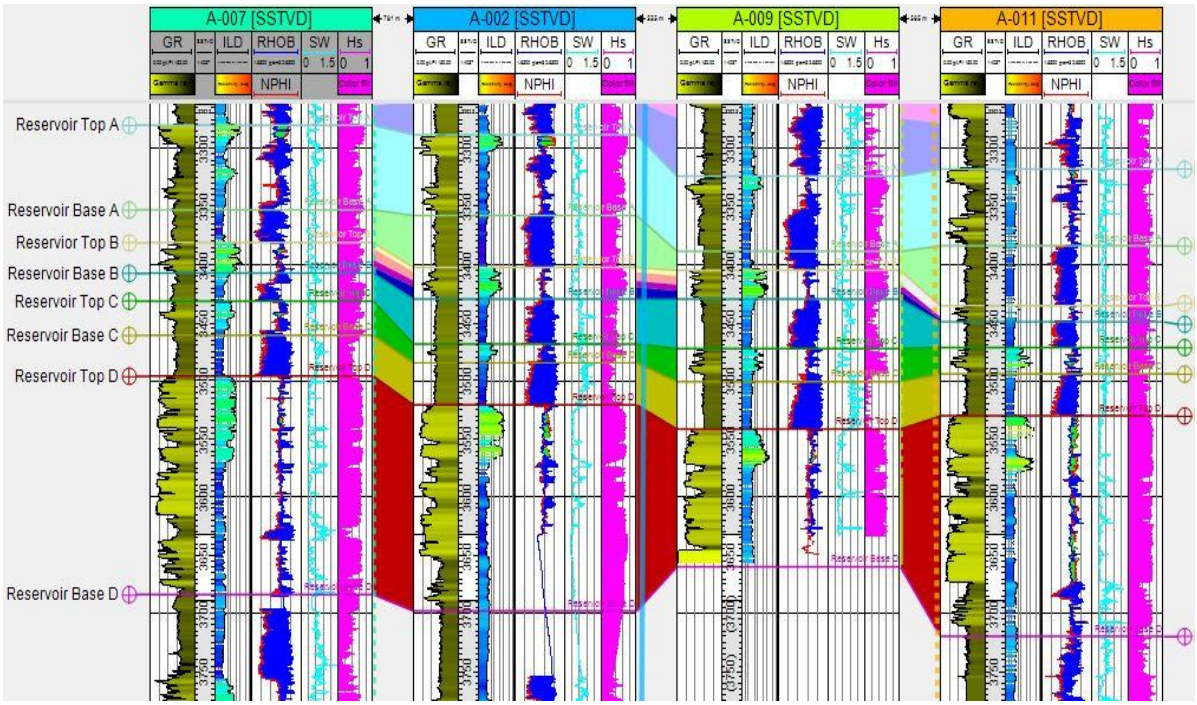

Fig. 11. Hydrocarbon saturation calculated for the four reservoir intervals and correlated across all four wells

5.10 Fluid Type

The three possible fluids that can exist in the pore spaces of reservoirs which accumulated over time due to migration, timing, good sealing mechanism and a trap formed from its source, are oil, gas, water (fresh or brine) or a combination of any two. The he presence of oil and water in the reservoirs was determined using the resistivity log, due to the fact that oil is more resistive than water. In this study, reservoir A is oil and water bearing in well A-002, A-011 and Oil bearing in A-007, A-009, while reservoir B is oil and water bearing in all the wells (Table 2). Reservoir C, is oil and water bearing in A-002, A-009, while A-007and A-011 are oil bearing only,

while in reservoir D, wells A-002, A-007, A-009, and A-011 are all oil and water bearing. Thus, we can summarized that all the reservoir intervals are hydrocarbon bearing and can be produced.

5.11 Fluid Saturation

The fluids saturation in the reservoirs was determined using Archie's equation and the logs generated are presented in Fig. 11. Water saturation calculated for reservoir A are 59% in A-002 well, 42% in A-007, 35% in A-009 and 78% in A-011 well. This accounts for an equivalent hydrocarbon saturation of 41%, 58%, 65% and 22% respectively (Table 2). For reservoir B, water saturation is 56% in A-002, 52% in A-007, 66% in A-009 and 51% in A-011 well, resulting in an equivalent hydrocarbon saturation of 44%, 48%, 34% and 49% respectively. In reservoir C, water saturation

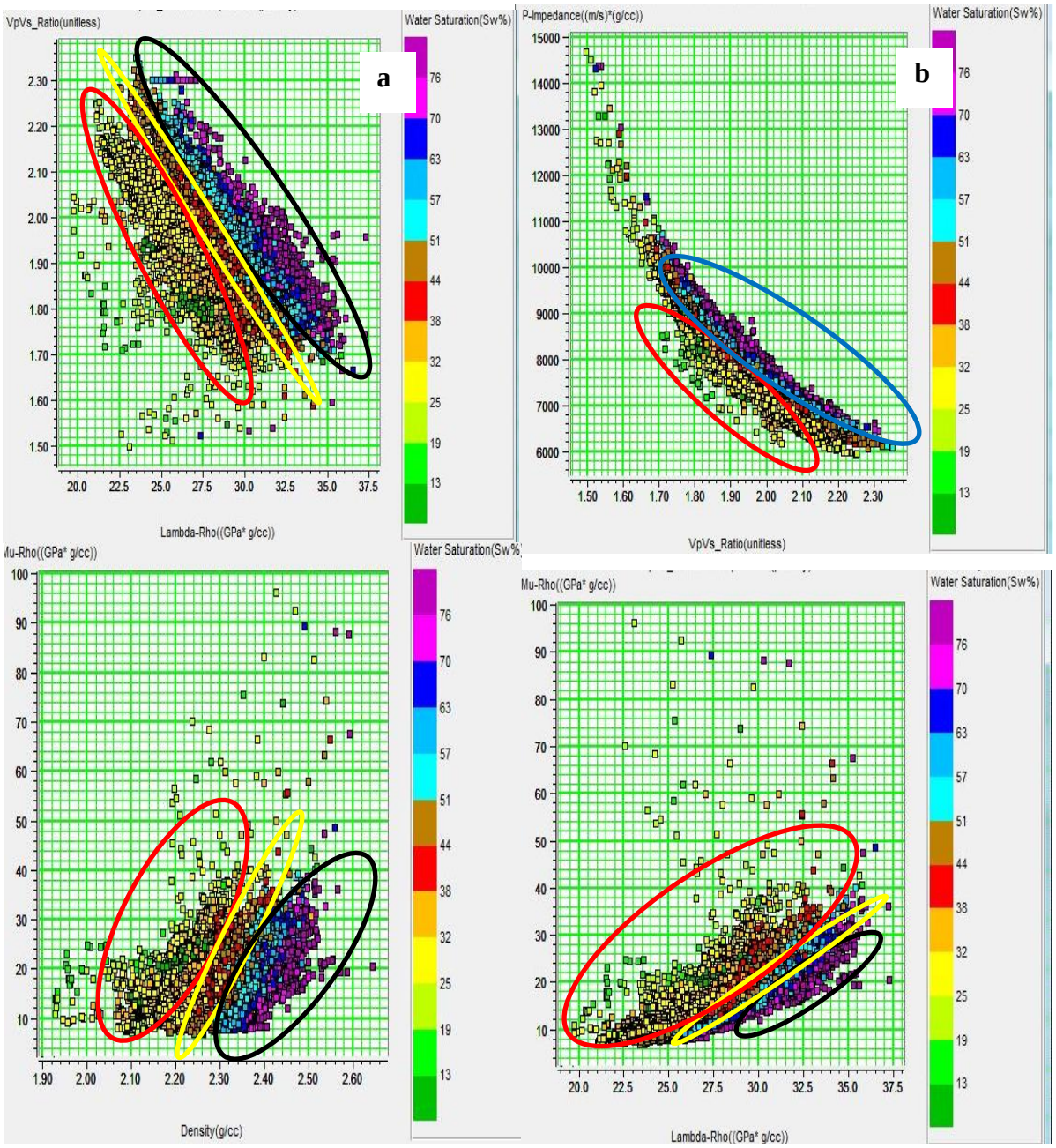

Fig. 12. Cross plots for attributes computed to identify lithology and fluid discrimination using water saturation colour for Well 11

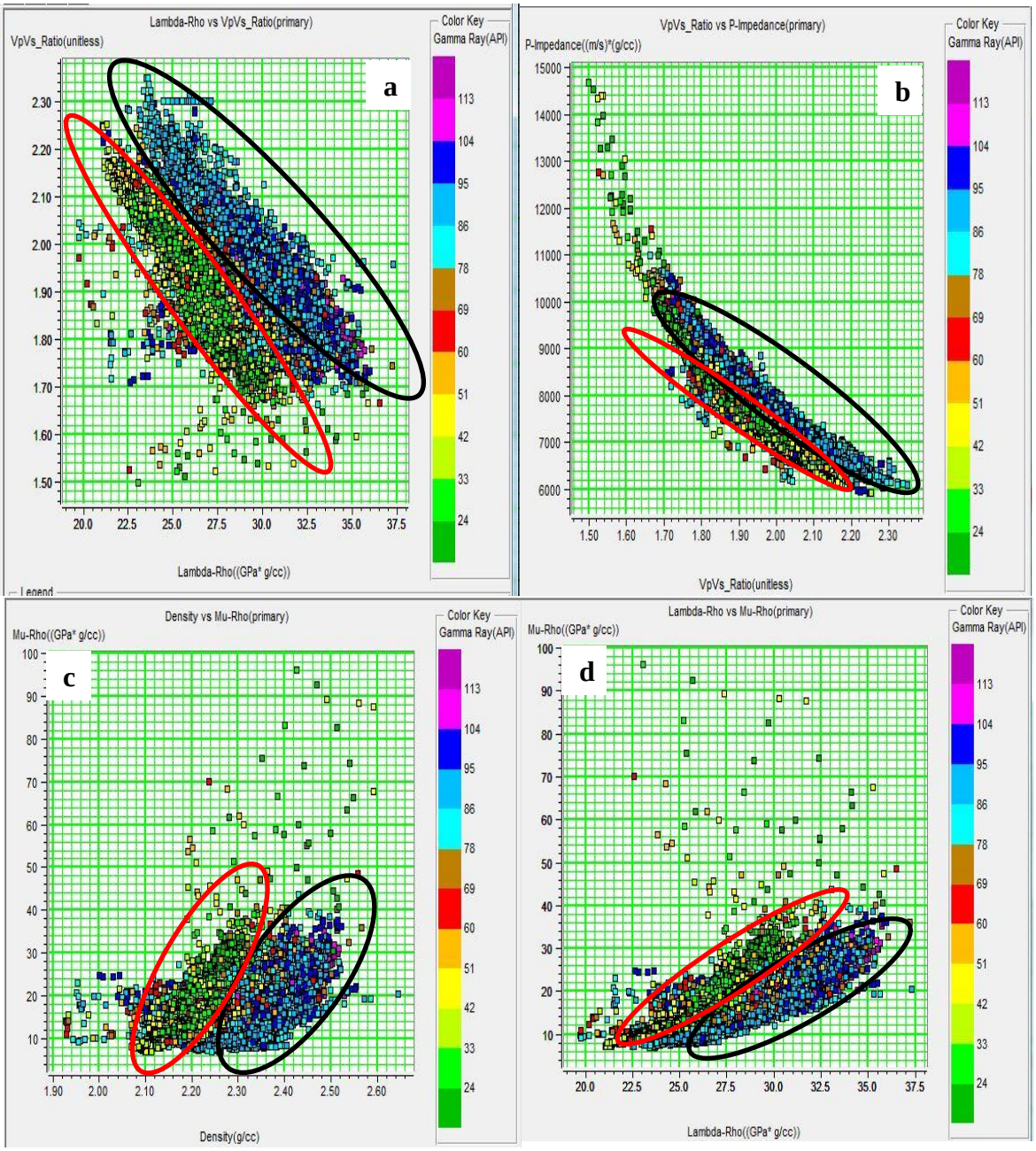

Fig. 13. Cross plots for attributes computed to identify lithology discrimination using gamma ray colour key for Well 11

values are 82%, 41%, 56% and 44% in A-002, A-007, A-009, and A-011 wells respectively. Accordingly, hydrocarbon saturation in reservoir C is as follows; 18%, 59%, 28% and 56% respectively, while in reservoir D, water saturation computed were 78%, 82%, 76% and 81% in A-002, A-007, A-009, and A-011 wells and the corresponding hydrocarbon saturation are 22%, 18%, 24% and 19% in A-002, A-007, A-009, and A-011 wells. The average hydrocarbon saturation values for reservoirs the reservoirs A, B, C and D are 46.5%, 43.75%, 40.25% and 20.75% respectively. These results show that reservoir A has the highest hydrocarbon saturation while reservoir D has the least hydrocarbon saturation measurement (Fig. 11) and Table 2.

5.12 Lithology and Fluid Discrimination

The lithology and fluid contents of the reservoir were discriminated using the cross plotting analysis, some selected rock properties and rock attributes were used and the following results

obtained. Firstly, a cross plot of Vp/Vs ratio against acoustic impedance was used to distinguished reservoir sand unit A-011 into sand zone, shaly-sand zone, and shale zone. While the cross plot of lambda-rho (incompressibility) against Vp/Vs helps to discriminates the target reservoir of interest into sands and shale/sand/shale sequences. Also the cross plot of Mu-rho against density was plotted, and finally, the cross plots of lambda-rho (λρ) against mu-rho (μρ), which help to distinguished the reservoir into four zones, which can be classified as probable shale, brine, and gas zone.

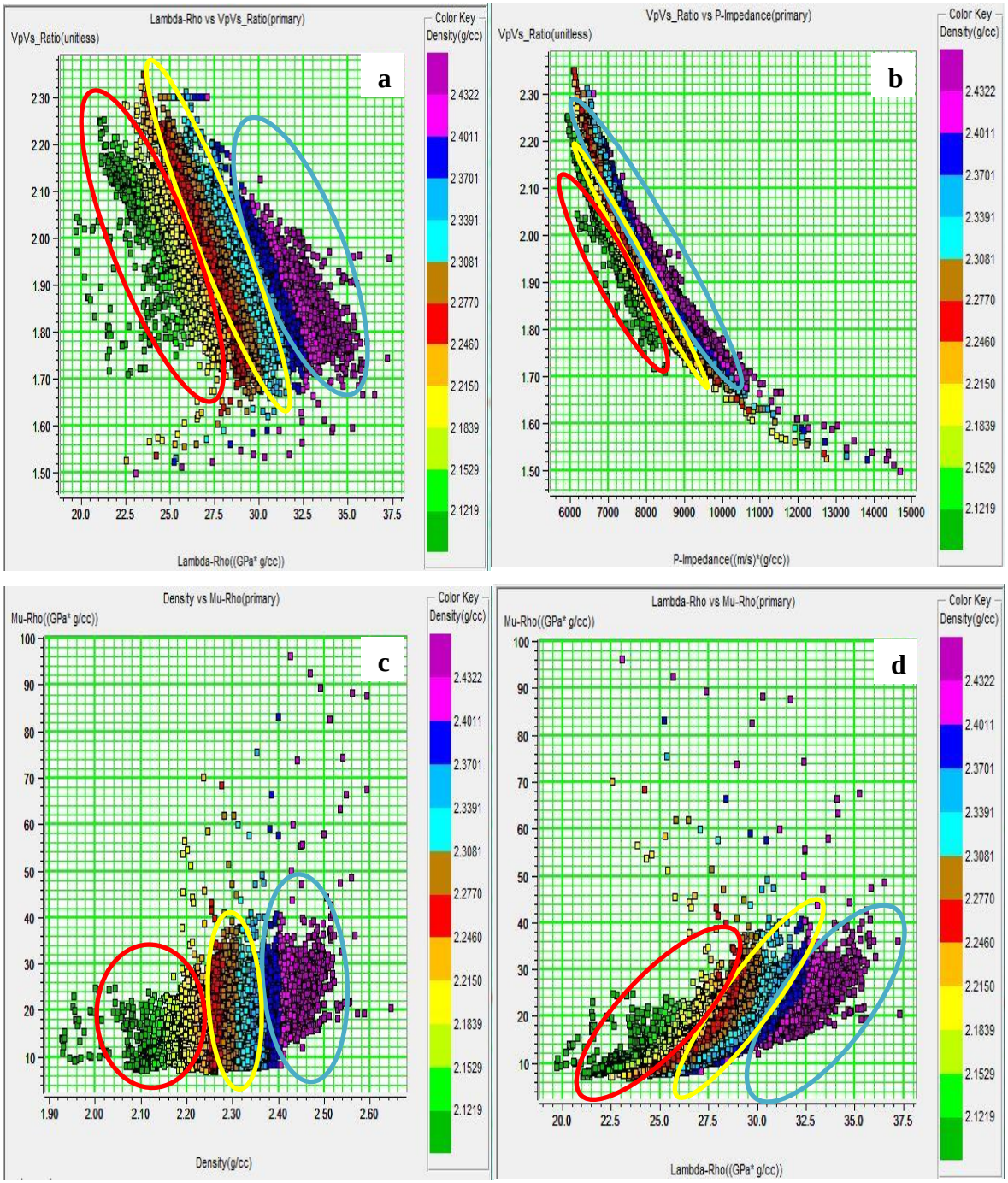

Fig. 14. Cross plots for attributes computed to identify fluid and lithology discrimination using density colour key for Well 11

6. DISCUSSION

6.1 Petrophysical Reservoir Analyses

Figs. 6a-d and 7 shows the mapped reservoirs in wells, with the associated petrophysical parameter logs while Table 2 gives a summary of the reservoir details encountered in the well.

The four main reservoir units were identified (namely reservoirs A, B, C and D) across the wells (Figs. 7, 8, 9, 10 and 11). The reservoir sand units range from about 16m to 177m thickness in Well A-002, 26m to 188m thickness in Well A-007, 26m to 118m thickness in Well A-009 and from 14m to 189m thickness in Well A-011 respectively. These reservoir units are generally made up of fairly clean sands, with an average shale volume that ranges from about 12.75% to 18.5%, average total and effective porosity ranging from 18.5% to 25.75% and 16.75% to 22.5% respectively, while the average water saturation ranges from about 54.25% to 68.75%. Reservoirs A and D shows signatures depicting block with sharp top and base sequence, reservoirs B show signatures depicting a fining downward with sharp base, while reservoir C show a coarsing upward with sharp top sequences on both ends of the shale beds. Reservoir B was observed to house the cleanest sand unit within the reservoirs.

6.2 Cross Plots Analysis

From the results obtained, both mu-rho and density can be classified as lithology discriminators, the Mu-rho values are normally high for sand bodies and low for shale units, while density is the reverse where shale has higher density value than that of sand. Fig. 12a, shows the results obtained for the plot of the variation of lambda-rho (incompressibility) against Vp/Vs, for sands and shale/sand/shale sequences. The lambda-rho (λρ) are better lithology discriminator tool because the cross plots are better aligned towards the lambda rho axis. The black ellipse rings distinguishes the shale zone, the yellow indicates the brine sand, while the ellipse indicates hydrocarbon sand. Using the cross plot of Vp/Vs ratio against Acoustic impedance (Zp) as shown in Fig. 12b, the reservoir unit A-011was delineated into two distinguish zones namely; hydrocarbon sands (red ellipse), and shale zone (blue ellipse). The results from the cross plot shows this as an good fluid discriminator and lithology delineation tool along the acoustic impedance axis, which means that the acoustic impedance attribute can be used effectively to describe the A-011 reservoir conditions in terms of lithology and fluid content, when compare with the results for Vp/Vs ratio. In the cross plot of Mu-rho (μρ) against density (Fig. 12c), in which brine is considered denser than hydrocarbon (oil and gas), Then, the red ellipse in the Fig. 12c indicates hydrocarbon bearing sand, while the yellow ellipse shows the brine saturated sand region, and the black section describes the shale region. The cross plots of lambda-rho (λρ) against mu-rho (μρ) as shown in Fig. 12d, the reservoir is separated into four zones that can be easily classified as probable shale (black eclipse), brine (yellow eclipse), oil (red eclipse) and gas zone (blue eclipse) using the water saturation values (lowest). From the result of the cross plot, we can deduce that lambda-rho (λρ) is more robust than mu-rho (μρ) in the analysis of fluids contents for this study, because the values of mu-rho (μρ) are relatively low for the reservoir sand. From the results obtained, the Lambda-rho (λρ), Mu-rho (μρ), Acoustic impedance (Zp) and Poisson impedance (PI) attributes were found to be most robust in lithology and fluid discrimination within the reservoir for the cross-plot analysis. The lambda-Mu-Rho (λ-μ-ρ) technique was able to identify hydrocarbon sands, due to its ability to distinguish responses of both the lambda-rho (λρ) and Mu-rho (μρ) sections to hydrocarbon sands versus shale. Generally, most lithologies can be effectively identified by the use of the cross plot of lambda-rho (λρ) versus Mu-rho (μρ), based on the fact that each lithology has a different rock properties response depending on the fluid content and mineral properties within the reservoir unit. The cross plots for computed attributes for lithology discrimination using the plots of Vp/Vs ratio against lambda-rho (λρ), acoustic impedance (Zp) against Vp/Vs ratio, Mu-rho (μρ) against density and mu-rho (μρ) against lambda-rho (λρ) respectively are shown in Fig. 13, using Well 11 as the pilot example, the results depicts that in the reservoirs of study the lithologies are majorly sands and shale, which are predominantly found in Niger Delta area. For Fig. 14, shows the cross plots of Vp/Vs ratio against lambda-rho (λρ), Vp/Vs ratio against acoustic impedance (Zp), mu-rho (μρ) against density and mu-rho (μρ) against lambda-rho (λρ) respectively, the result shows that the reservoirs discriminates the blue eclipse as shale area, yellow eclipse as brine sands and red eclipse as oil respectively.

6.3 Vp/Vs Ratio against Lambda-rho

The cross plots of Vp/Vs ratio against Lambda-rho from petrophysical properties (gamma ray, water saturation and density) clearly show the

distinct discrimination of probable hydrocarbon zones from the brine/shale zones within well A-011 (Figs. 12a – 14a). From the cross plot, it was observed that the hydrocarbon zones correspond to low Lambda-Rho and high Vp/Vs ratio while brine/shale zones correspond to high Lambda-rho and low Vp/Vs ratio.

6.4 Vp/Vs Ratio against P-Impedance

The cross plots of P-impedance against Vp/Vs ratio from petrophysical properties (gamma ray, water saturation and density) clearly show the distinct discrimination of probable hydrocarbon sand zones from the shale zones within well A-011 (Figs. 12b - 14b). From the cross plot, it was observed that the hydrocarbon sand zones correspond to high P-impedance and low Vp/Vs ratio while shale zones correspond to low P-impedance and high Vp/Vs ratio respectively.

6.5 Mu-rho against Density

The cross plots of Mu-rho against density from petrophysical properties (gamma ray, water saturation and density) clearly show the distinct discrimination of probable hydrocarbon sand zones from the shale zones within well A-011 (Figs. 12c – 14c). From the cross plot, it was observed that the hydrocarbon sand zones correspond to high mu-rho and low density while shale zones correspond to low mu-rho and high density.

6.6 Mu-rho against Lambda-rho

The cross plots of Mu-rho against Lambda-rho from petrophysical properties (gamma ray, water saturation and density) clearly shows the distinct discrimination of probable hydrocarbon zones from the brine/shale zones within well A-011 (Figs. 12d – 14d). From the cross plot, it was observed that the hydrocarbon zones correspond to high mu-rho and low lambda-rho while brine/shale zones correspond to low mu-rho and high lambda-rho.

7. CONCLUSION

The study used the results obtained from the well logs evaluation, well log correlation, petrophysical analysis and the cross plots analysis, to delineate the lithology and discriminate the reservoir fluids in other to characterized our study area, A-Field, in an onshore Niger Delta Area. In the reservoir delineation, four lithological sand reservoir units were identified using the gamma ray log, resistivity log and the cross plot of neutron and density logs. The study evaluated the following petrophysical parameters for the field as follows, average effective porosity of 18.4%, total porosity estimated to be 20.25%, the average shale volume of 61.75%, average water saturation of 53.5% and permeability of 1508.0425mD respectively, these parameters were used to further quantify the extends of producibility of the four reservoirs.

Cross plots of computed extracted attributes were used to accurately delineate the lithology and discriminate the fluids, so as to further characterize the existence of fluid and lithology in the reservoir.

The quantitative interpretation of the reservoir characterization of A-field has revealed that the use of estimated petrophysical parameters of the rock properties as reservoir characterization technique was an effective technique, especially for fluid and lithology discrimination of the field in any given reservoir study. This study has also shown that A-field is not commercially viable in terms of hydrocarbon exploitation within the reservoir intervals studied because of the high-water saturation and shale volume values estimated, which are not highly economical for production of the field.

COMPETING INTERESTS

Authors have declared that no competing interests exist.

REFERENCES

1. Ajisafe YA. 3-D Seismic Attributes for Reservoir Characterization of Y Field Niger Delta, Nigeria. Journal of applied Geology and Geophysics (IOSR-JAGG). 2013;23-31.
2. Oyeyemi DK, Aizebeokhai PA. Seismic Attribute Analysis for Reservoir Characterization; Offshore Niger Delta. Petroleum and Coal. 2015;57(6):619-628.
3. Perveiz KN. An Integrated Seismic Interpretation and Rock Physics attributes analysis for pore fluid discrimination. Arabian Journal for Geoscience and Engineering. 2016;41(1):191-200.
4. Sofolabo AO, Ehirim CN, Dagogo T. Cross plot analysis of Extracted Seismic inversion attributes for fluid and Lithology discrimination: A case study of K-Field, Onshore Niger Delta Area, Nigeria. International Journal of Science and Research (IJSR). 2018;7(4):804-810.

5. Barnes AE. Seismic Attributes in your facies, Canadian Society of Exploration Geophysicists (CSEG) Recorder, Series. 2001;9:41-47.
DOI: 74.3.176.63.
6. Chen Q, Sidney S. Seismic Attribute Technology for Reservoir Forecasting and Monitoring. Geophysics, The Leading Edge. 1997;445-456.
7. Doust H, Omotsola E. Niger Delta. In: Edwards, J.D. and Santogrossi, P.A., Eds., Divergent/Passive Margin basins. American Association of Petroleum Geologists,(AAPG) Bulletin. 1990;239-248. Available:https://doi.org/10.1306/M48508C4
8. Opara AI, Anyiam UO, Nduka AV. 3D Seismic Interpretation and Structural Analysis of Ossu Oil Field, Northern Depobelt, Onshore Niger Delta, Nigeria. The Pacific Journal of Science and Technology. 2011;12(1):8.
9. Tuttle MLW, Charpentier RR, Brownfield ME. The Niger delta petroleum system: Niger delta province, Nigeria, Cameroon, and Equatorial Guinea, Africa. 1999;99-50.
10. Weber KJ. Petroleum Geology of the Niger Delta:. Proceedings of the Ninth World Petroleum Congress, 2, Geology: London: Applied Science Publishers, Ltd. 1975;210-221
11. Evamy BO, Herembourne J, Kameline P, Knap WA, Molloy FA, Rowlands PH. Hydrocarbon habitat of Tertiary Niger Delta. American Association of Petroleum Geologists Bulletin. 1978;62:1-39.
12. Short K, Stauble AJC. Outline of Geology of the Niger delta, The American Association of Petroleum Geologists Bulletin. 1967;51:761–779.
13. Weber KJ. Hydrocarbon distribution patterns in Nigerian growth fault structures controlled by structural style and stratigraphy. American Association of Petroleum Geologists (AAPG) Bulletin. 1986;70:661-662.
14. Stacher P. Present understanding of the Niger delta hydrocarbon habitat: Geology of Deltas. AA Balkema, Rotterdam. 1995;257–267.
15. Reijers TP. The Niger Delta Basin,. Elsevier Science. 1997;151-172.
16. Corrodor F, Shaw JH, Billoti F. Structural styles in the deep-water fold and thrust belts of the Niger Delta. American Association of Petroleum Geologists Bullettin (AAPG), Tulsa. 2005;89:753-780.
17. Daukoru CM. Northern Delta Depobelt Portion of the Akata-Agbada Petroleum system, Niger Delta, Nigeria, Petroleum Association System, AAPG memoir 60. American Association of Petroleum Geologists, Tulsa (AAPG). 1994;598-616.
18. Nwachukwu SO. The tectonic evolution of the Southern portion of the Benue trough . Geological Magazine. 1972;109(5):411-419.
19. Olowokere MT, Ojo JS. Fluid Detections and Lithology Discrimination using Lame Petrophysical Parameters from Simultaneous Inversion – using Northern North Sea, Norway. National Association of Petroleum Explorationists (NAPE) Int'l Bulletin. 2010;22(1):36-42.
20. Ekweozor CM. Petroleum Source-Bed Evaluation of Tertiary Niger Delta; American Association of Petroleum Geologists Bulletin (AAPG) Bulletin. 1984; 68:387-394.
21. Schlumberger. Log Interpretation Principle/Applications. Texas, USA. 1989; 1-241.
22. Cannon S. Rock and Fluid Properties. In Petrophysics, S. Cannon (Ed.); 2015. Available:https://doi.org/10.1002/9781119117636.ch3.
23. Hilchie DW. Applied Openhole Log Interpretation (For Geologists and Petroleum Engineers). 1st Ed, Geophysical Well Logging, Golden Publishing, Colorado, USA. 1978;1-350.
24. Archie GE. The Electrical Resistivity Log as an Aid in determining Some Reservoir Characteristics. Petroleum Transactions of the American Institute of Mining, Metallurgical and Petroleum Engineering (AIME). 1942;146:54-62.
25. Owolabi OO, Long John TF, Ajienka JA. An empirical expression for permeability in Unconsolidated Sands of the Eastern Niger Delta. Journal of Petroleum Geology. 1994;17(1)111-116.
26. Larionov VV. Borehole Radiometry: Nedra, Moscow, USSR; 1969.
27. Aamir R, David WE, McDougall A, Pedersen PK. Reservoir Characterization Using Microseismic Facies Analysis Integrated with surface seismic attribute, SEG The Leading Edge. 2016;4(2):1-260.
28. Adel AA. Seismic Attributes Techniques to delinate channel complex in pliocene age, North Abu Qir, Nile Delta. Eygpt Journal of applied science Research. 2013;10(2): 4255-4270.

29. Aizebeokhai KD. Seismic Attributes Analysis For Reservoir Characterization; Offshore Niger Delta. Petroleum & Coal. 2015;57(6):619-628.
30. Anyiam UO. 3D Seismic Attribute Expressions of Deep Offshore Niger Delta, Master of Science Thesis, Federal University of Technology Owerri, Nigeria; 2008.
31. Austin Oyinkuro O, Opukumo AW. Petrophysical Analysis of Some Hydrocarbon Reservoirs in Eastern Niger Delta Basin Using Well Logs. IOSR Journal of Applied Geology and Geophysics (IOSR-JAGG). 2021;9(6)1:41-51. Available:https://doi.org/10.9790/0990-0906014151
32. Bello R, Igwenagu CL, Onifade Y. Cross plotting of Rock Properties for Fluid and Lithology Discrimination using Well. Journal of Applied Science, Environnment and Manage. 2005;539-546.
33. Brown AR. Interpretation of Three-Dimensional Seismic Data, Society of Exploration Geophysicists and American Association of Petroleum Geologists, 6th edition; 2011.
34. Iske A, Randen T. Mathematical Methods and Modeling in Hydrocarbon exploration and Production. Schlumberger, Springer Publication; 2005.
35. Lowrie W. Fundamentals of Geophysics. London: Cambriodge University Press; 2007.
36. Omudu LM, Ebeniro JO, Osayande N. Cross-plot and Discriptive Statistic for Lithology and Fluid Discrimination – A case study from Onshore Niger Delta. National Association of Petroleum Explorationists (NAPE) International Bulletin. 2008;20(2): 31-37.
37. Omudu LM, Ebeniro JO, Xynoglass M, Osayande N. Fluid Discriminator Factor, Moduli Ratio and Reservior Characterization – A Niger Delta Experience. National Association of Petroleum Explorationists (NAPE) International Bulletin. 2008;20(2):38-44.
38. Russell BH, Hedlin K, Hitterman FJ, Lines LR. Fluid property discrimination with AVO, A Biot- Grassmann perspective. Geophysics. 2003;68:29-39.
39. Sheriff RE, Telford WM, Geldart LP. Applied Geophysics 2nd Ed, Cambridge University Press; 1980.
40. Subrata B, Sunil S, Prabir N, Afrah A, Sarah A, Abdulaziz A. Identification of Thin Carbonate Reservoir Facies through Integrated Seismic Attribute Analysis: A Case Study of Kuwait, The Leading Edge SEG. 2017;6093.
41. Van Bemmel PP, Pepper REF. Seismic signal processing method and apparatus for generating a cube of variance values. U.S Patent. 2000;6(151):555.
42. Weber KJ, Daukoru EM. Petroleum Geology of the Niger Delta; Earth Science Journal. 1975;2(1):210-221.